INTERNATIONAL JOURNAL FOR NUMERICAL METHODS IN FLUIDS
Int. J. Numer. Meth. Fluids **31**: 17–36 (1999)

A POSTERIORI FINITE ELEMENT ERROR BOUNDS FOR NON-LINEAR OUTPUTS OF THE HELMHOLTZ EQUATION

J. SARRATE[a,*], J. PERAIRE[a] AND A. PATERA[b]

[a] *Department of Aeronautics and Astronautics, Massachusetts Institute of Technology, Cambridge, MA 02139, USA*
[b] *Department of Mechanical Engineering, Massachusetts Institute of Technology, Cambridge, MA 02139, USA*

SUMMARY

A Neumann subproblem *a posteriori* finite element procedure for the efficient and accurate calculation of rigorous, constant-free upper and lower bounds for non-linear outputs of the Helmholtz equation in two-dimensional exterior domains is presented. The bound procedure is firstly formulated, with particular emphasis on appropriate extension to complex-valued equations; then, illustrative numerical examples for outputs, such as the intensity of the scattered wave over a small segment of the domain boundary, are provided. Copyright © 1999 John Wiley & Sons, Ltd.

KEY WORDS: FE error bounds; Helmholtz equation; non-linear outputs

1. INTRODUCTION

Over the past two decades, engineering applications that involve the solution of the Helmholtz equation in exterior domains—scattering wave problems—have become increasingly important. These applications range from low-frequency problems, such as sea-wave propagation in inner ports [1], to high-frequency problems, such as the prediction of the radar scattering cross-section of complex objects and vehicles [2–4].

Several numerical techniques can be used to solve these challenging problems. For homogeneous media, boundary integral methods [5–7] are probably the most prevalent. These techniques automatically satisfy the radiation condition at infinity, furthermore, they reduce the effective spatial dimension of the problem, which in turn leads to significant computational economies. However, recent developments in the field of approximate boundary conditions, infinite elements and iterative solvers [8–10] have rendered the finite element method competitive, especially for non-homogeneous media. Critical questions remain, however, in particular as regards accuracy and appropriate meshes.

In general, the accuracy of a finite element solution of a partial differential equation can be predicted by *a priori* and *a posteriori* error estimators. *A priori* error estimates can be readily found even for non-coercive problems, such as the Helmholtz equation, in, for example, the H^1 and L^2 norms [3,11]. Although these estimates reveal the correct asymptotic rate of convergence, their application to practical computations is limited since the estimates involve norms

* Correspondence to: Department de Matemàtica Aplicada III, Universitat Politècnica de Catalunya, Gran Capitan s/n, Modul C2, Barcelona, 08034, Spain.

CCC 0271–2091/99/170017–20$17.50

of the unknown solution. *A posteriori* procedures overcome this problem by expressing the error in terms of the computed numerical solution. *A posteriori* error estimators in the H^1 and L^2 norms are available for the Helmholtz equation [4,12–14]; these estimators form the basis for effective adaptive procedures.

However, from the engineering point of view, it is more advantageous and interesting to develop *a posteriori* estimators for error metrics more directly relevant to engineering analysis. In particular, the quantity (or quantities) of interest in engineering studies is typically not the field variable u or the error in the energy norm, but rather the outputs (e.g. the flux across a boundary, the normal force on a surface, or the mean value of the solution) that reflect the specific goals and objectives of the design or optimization process. Moreover, engineers may be at least as interested in prediction confirmation as in adaptivity: it is thus essential that all constants be evaluated, and explicit techniques [15] are therefore less attractive than implicit procedures.

In References [16–19], a general formulation for *a posteriori* bounds for output functionals of rather general partial differential equations are developed. This formulation relies on previous developments in implicit (subproblem) *a posteriori* theory, in particular the application of quadratic–linear duality theory [20,21] and the construction of equilibrated hybrid fluxes [20–22]. However, the critical discriminator and advantage of this approach is that rigorous, accurate and quantitative (constant-free) bounds are obtained directly for the engineering quantities of interest, rather than the energy norm or energy norm equivalents [23].

Initially, the formulation was applied to symmetric and coercive problems (the Poisson equation and linear elasticity) [18], non-symmetric coercive problems (e.g. the convection–diffusion equation) [18], certain constrained problems (e.g. the Stokes equations) (M. Paraschivoiu and A.T. Patera, '*A posteriori* bounds for linear-functional outputs of Crouzeix–Raviart finite element discretizations of the incompressible Stokes problem', *Int. J. Numer. Methods Fluids*, submitted), and non-coercive problems that satisfy a Garding inequality [11] (e.g. the Helmholtz equation for interior domains) [24]. Recently, a more general formulation has been developed [16,25], which not only includes these previous cases, but also non-linear outputs and non-linear equations (e.g. the eigenvalue problem and the Burgers equation). The goal in this paper is to extend the earlier work for the one-dimensional real-valued interior Helmholtz problem to the much more challenging, and relevant, multi-dimensional complex-valued exterior Helmholtz problem. Attention shall be restricted here to confirmation of (non-linear) outputs: future papers will consider the development of local error indicators and associated adaptive strategies following the formulation described in [19].

This paper is organized as follows. In Section 2, the strong and the weak forms of the problem are stated. In Section 3, several space definitions are introduced; the bound estimator procedure is then described; and finally, the requisite bounding properties are demonstrated. In Section 4, several numerical examples are presented. Brief conclusions are given in Section 5.

2. PROBLEM STATEMENT

2.1. Strong formulation

Given an incident wave, we are interested in the computation of outputs that are non-linear functionals of the resulting scattered wave. The strong form for the scattered wave in a homogeneous medium can be stated as: find $\tilde{u}$: $\bar{\Omega} \rightarrow \mathbb{R}$ such that

$$\frac{1}{c^2}\frac{\partial^2 \tilde{u}}{\partial t^2} - \nabla^2 \tilde{u} = \tilde{f} \quad \text{in } \Omega, \tag{1}$$

$$\tilde{u} = \tilde{g}^{\mathrm{D}} \quad \text{on } \Gamma_{\mathrm{D}}, \tag{2}$$

$$\frac{\partial \tilde{u}}{\partial n} = \tilde{g}^{\mathrm{N}} \quad \text{on } \Gamma_{\mathrm{N}}, \tag{3}$$

$$\frac{\partial \tilde{u}}{\partial n} = -\frac{1}{c}\frac{\partial \tilde{u}}{\partial t} \quad \text{on } \Gamma_{\mathrm{R}}, \tag{4}$$

where c is the wave velocity, $\tilde{f}$: $\bar{\Omega} \to \mathbb{R}$ is the source term, and $\tilde{g}^{\mathrm{D}}$: $\Gamma_{\mathrm{D}} \to \mathbb{R}$ and $\tilde{g}^{\mathrm{N}}$: $\Gamma_{\mathrm{N}} \to \mathbb{R}$ are Dirichlet and Neumann data respectively; here $\partial \tilde{u}/\partial n = \nabla \tilde{u} \cdot \hat{\mathbf{n}}$, where $\hat{\mathbf{n}}$ is the outward unit normal on the boundary. It is important to note that the radiation condition on Γ_{R} is only approximate; higher-order forms can be developed but will not be pursued in this paper. It is assumed that the boundary Γ verifies

$$\Gamma = \overline{\Gamma_{\mathrm{D}} \cup \Gamma_{\mathrm{N}} \cup \Gamma_{\mathrm{R}}}, \tag{5}$$

$$\varnothing = \Gamma_{\mathrm{D}} \cap \Gamma_{\mathrm{N}} = \Gamma_{\mathrm{D}} \cap \Gamma_{\mathrm{R}} = \Gamma_{\mathrm{N}} \cap \Gamma_{\mathrm{R}}, \tag{6}$$

as shown in Figure 1.

Assuming harmonic data of the form $\tilde{f} = \Re\{f\, \mathrm{e}^{\mathrm{i}\omega t}\}$, $\tilde{g}^{\mathrm{D}} = \Re\{g^{\mathrm{D}}\, \mathrm{e}^{\mathrm{i}\omega t}\}$ and $\tilde{g}^{\mathrm{N}} = \Re\{g^{\mathrm{N}}\, \mathrm{e}^{\mathrm{i}\omega t}\}$ (where $\Re\{v\}$ denotes the real part of v, and $\mathrm{i} = \sqrt{-1}$), the *stationary* solution of the above problem will be of the form $\tilde{u} = \Re\{u\, \mathrm{e}^{\mathrm{i}\omega t}\}$. The strong statement for the resulting complex Helmholtz equation is thus: find u: $\bar{\Omega} \to \mathbb{C}$ such that

$$-\nabla^2 u - k^2 u = f \quad \text{in } \Omega, \tag{7}$$

$$u = g^{\mathrm{D}} \quad \text{on } \Gamma_{\mathrm{D}}, \tag{8}$$

$$\frac{\partial u}{\partial n} = g^{\mathrm{N}} \quad \text{on } \Gamma_{\mathrm{N}}, \tag{9}$$

$$\frac{\partial u}{\partial n} = -\mathrm{i}ku \quad \text{on } \Gamma_{\mathrm{R}}, \tag{10}$$

where $k = \omega/c$ is the wave number. The output s is evaluated as a functional of the field variable u; this is described in greater detail in the next subsection.

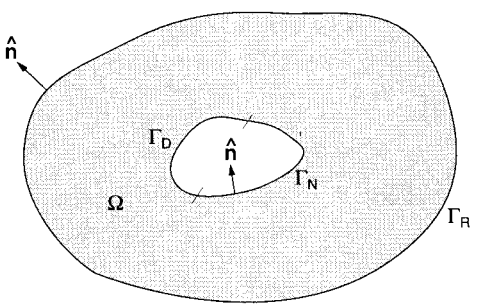

Figure 1. General geometry and boundary conditions for the complex Helmholtz problem.

2.2. Weak formulation

We first introduce the space

$$\tilde{Z}(\mathscr{D}) = \{v = v^{\mathrm{R}} + \mathrm{i}v^{\mathrm{I}}:\ v^{\mathrm{R}} \in H^1(\mathscr{D}),\ v^{\mathrm{I}} \in H^1(\mathscr{D})\}, \tag{11}$$

where $H^1(\mathscr{D})$ is the usual Sobolev space [26] associated with a domain $\mathscr{D} \subset \mathbb{R}^2$. Here and throughout this paper, superscripts R and I denote the real and imaginary part respectively, i.e. $v^{\mathrm{R}} = \Re(v)$ and $v^{\mathrm{I}} = \Im(v)$; $\bar{v}$ shall denote the complex conjugate of v, and $|v|$ the modulus of v. Then the sets

$$Z = \{v \in \tilde{Z}(\Omega):\ v|_{\Gamma_{\mathrm{D}}} = 0\}, \tag{12}$$

$$Z^{\mathrm{D}} = \{v \in \tilde{Z}(\Omega):\ v|_{\Gamma_{\mathrm{D}}} = g^{\mathrm{D}}\}, \tag{13}$$

which reflect the essential boundary conditions, are introduced.

Under these definitions, the weak formulation of the Helmholtz problem is: find $u \in Z^{\mathrm{D}}$ such that

$$\mathscr{A}(u, v) = 0, \quad \forall v \in Z, \tag{14}$$

where the form $\mathscr{A}$: $\tilde{Z}(\Omega) \times \tilde{Z}(\Omega) \to \mathbb{C}$ is defined as

$$\mathscr{A}(u, v) = a(u, v) - m(u, v) + \mathrm{i}p(u, v) - \langle f, v \rangle - \langle g^{\mathrm{N}}, v \rangle_{\mathrm{N}}. \tag{15}$$

Here the bilinear forms are given by

$$a(w, v) = \int_{\Omega} \nabla w \cdot \nabla \bar{v}\ \mathrm{d}\Omega, \tag{16}$$

$$m(w, v) = k^2 \int_{\Omega} w\bar{v}\ \mathrm{d}\Omega, \tag{17}$$

$$p(w, v) = k \int_{\Gamma_{\mathrm{R}}} w\bar{v}\ \mathrm{d}\Gamma, \tag{18}$$

and the duality pairings by (assuming sufficient smoothness)

$$\langle f, v \rangle = \int_{\Omega} f\bar{v}\ \mathrm{d}\Omega, \tag{19}$$

$$\langle g^{\mathrm{N}}, v \rangle_{\mathrm{N}} = \int_{\Gamma_{\mathrm{N}}} g^{\mathrm{N}}\bar{v}\ \mathrm{d}\Gamma. \tag{20}$$

It is noted that $a(\cdot, \cdot)$ is Hermitian positive-definite.

Finally, we are interested in real outputs, s, that are non-linear functionals of the solution $u = u^{\mathrm{R}} + \mathrm{i}u^{\mathrm{I}}$. More precisely, we set: $s = \Re\{S(u)\}$, where $S(u)$: $\tilde{Z}(\Omega) \to \mathbb{C}$. Specific examples will be presented later in the paper.

3. ERROR BOUND FORMULATION

This section presents a procedure to obtain sharp bound estimators for non-linear outputs of the complex Helmholtz equation. In particular, the general formulation developed in [16–19] is extended to the complex-valued case.

3.1. Space definitions

We first introduce the finite element approximation subspaces. For the error bound procedure, two triangulations of Ω are considered: a working mesh $\mathscr{T}_H$, and a truth mesh $\mathscr{T}_h$. It is required that $\mathscr{T}_h$ is a refinement of $\mathscr{T}_H$ in the sense that any element, T_h, of $\mathscr{T}_h$ lies entirely within a single element, T_H, of $\mathscr{T}_H$. The standard piecewise–linear finite element sets can then be defined.

$$Z_\delta = \{v = v^{\mathrm{R}} + \mathrm{i}v^{\mathrm{I}}:\ v^{\mathrm{R}}|_{T_\delta} \in \mathbf{P}_1(T_\delta),\ v^{\mathrm{I}}|_{T_\delta} \in \mathbf{P}_1(T_\delta),\ \forall T_\delta \in \mathscr{T}_\delta\} \cap Z, \tag{21}$$

$$Z_\delta^{\mathrm{D}} = \{v = v_{\mathrm{R}} + \mathrm{i}v^{\mathrm{I}}:\ v^{\mathrm{R}}|_{T_\delta} \in \mathbf{P}_1(T_\delta),\ v^{\mathrm{I}}|_{T_\delta} \in \mathbf{P}_1(T_\delta),\ \forall T_\delta \in \mathscr{T}_\delta\} \cap Z^{\mathrm{D}}, \tag{22}$$

where $\mathbf{P}_1(T_\delta)$ is the space of linear polynomials over element T_δ. The working discretization corresponds to $\delta = H$, whereas the truth discretization corresponds to $\delta = h$. Note that $Z_H \subset Z_h \subset Z$, and furthermore, $Z_H^{\mathrm{D}} \subset Z_h^{\mathrm{D}} \subset Z^{\mathrm{D}}$ (it is assumed that g^{D} is sufficiently simple).

The working approximation $u_H \in Z_H^{\mathrm{D}}$ can be defined from

$$\mathscr{A}(u_H, v) = 0, \quad \forall v \in Z_H, \tag{23}$$

and thus, $s_H = \Re\{S(u_H)\}$. Similarly, for the truth mesh, $u_h \in Z_h^{\mathrm{D}}$ satisfies

$$\mathscr{A}(u_h, v) = 0, \quad \forall v \in Z_h, \tag{24}$$

with $s_h = \Re\{S(u_h)\}$. It is assumed that problem (23) can be solved at modest cost. It is further assumed that Z_h (the truth discretization) is sufficiently fine that S_h differs negligibly from s; this suggests that direct computation of s_h will be prohibitively expensive—hence the interest in bounds.

In order to apply the error bound procedure developed in [16,18,19], additional spaces and bilinear forms need to be defined. First, the *broken spaces* are defined with respect to the domain decomposition induced by Z_H as

$$\hat{Z}_\delta = \{v|_{T_H} \in \tilde{Z}(T_H),\ \forall T_H \in \mathscr{T}_H:\ v^{\mathrm{R}}|_{T_\delta} \in \mathbf{P}_1(T_\delta),\ v^{\mathrm{I}}|_{T_\delta} \in \mathbf{P}_1(T_\delta),\ \forall T_\delta \in \mathscr{T}_\delta\}. \tag{25}$$

Second, the set of open edges of the triangulation $\mathscr{T}_H$ is denoted by $\mathscr{E}(\mathscr{T}_H)$ and a space of functions defined over the element edges $\gamma \in \mathscr{E}(\mathscr{T}_H)$ is introduced,

$$\mathscr{Q}_H = \{q = q^{\mathrm{R}} + \mathrm{i}q^{\mathrm{I}}:\ q^{\mathrm{R}}|_\gamma \in \mathbf{P}_1(\gamma),\ q^{\mathrm{I}}|_\gamma \in \mathbf{P}_1(\gamma),\ \forall \gamma \in \mathscr{E}(\mathscr{T}_H),\ \text{and}\ q|_{\Gamma_{\mathrm{N}}} = q|_{\Gamma_{\mathrm{R}}} = 0\}. \tag{26}$$

Finally, the continuity bilinear form is defined as b: $\hat{Z}_h \times \mathscr{Q}_H \to \mathbb{C}$ as

$$b(v, q) = \sum_{\gamma \in \mathscr{E}(\mathscr{T}_H)} \int_\gamma [\bar{v}]_\gamma q|_\gamma \, \mathrm{d}\Gamma, \tag{27}$$

where $[v]_\gamma$ is the jump in v across γ when γ is in the interior, and the trace of v on γ when γ is on the boundary Γ. It is important to note that the form $b(\cdot, \cdot)$ can be exploited to enforce continuity, for example,

$$Z_H = \{v \in \hat{Z}_H:\ b(v, q) = 0,\ \forall q \in \mathscr{Q}_H\}. \tag{28}$$

Conversely, for any continuous function v that satisfies the homogeneous essential boundary conditions, and any function $q \in \mathscr{Q}_H$, $b(v, q) = 0$.

3.2. Bound procedure

The goal is to find, based solely on computations on the working space Z_H and *decoupled calculations* on the *broken* space $\hat{Z}_h$, lower and upper estimators that provide lower and upper bounds for $S(u_h)$ for H sufficiently small.

We first define

$$E(w, v) \equiv a(w, v) - m(w, v) + \mathrm{i}p(w, v); \tag{29}$$

E is further decomposed into its Hermitian and skew-Hermitian parts, $E = E^s + E^a$,

$$E^s(w, v) \equiv \frac{1}{2}\{E(w, v) + \overline{E(v, w)}\} = a(w, v) - m(w, v), \tag{30}$$

$$E^a(w, v) \equiv \frac{1}{2}\{E(w, v) - \overline{E(v, w)}\} = \mathrm{i}p(w, v); \tag{31}$$

finally, the Hermitian part is decomposed as $E^s \equiv E^s_Y + E^s_M$, where

$$E^s_Y(w, v) \equiv a(w, v), \tag{32}$$

$$E^s_M(w, v) \equiv -m(w, v). \tag{33}$$

Note that $E^s_Y(\cdot, \cdot)$ is positive-definite.

For the purposes of this paper, attention shall be restricted to linear and quadratic outputs; more general non-linear forms are readily treated, as described in [16]. The non-linear output functional may be expanded as

$$S(u_H + w) = S(u_H) + \ell^{\mathscr{O}}(w) + \mathscr{M}(w, w), \tag{34}$$

where $\ell^{\mathscr{O}}$: $\tilde{Z}(\Omega) \to \mathbb{C}$ and $\mathscr{M}$: $\tilde{Z}(\Omega) \times \tilde{Z}(\Omega) \to \mathbb{C}$ are the linear and bilinear contributions respectively [16]. It shall be required that $\mathscr{M}$ be L^2-continuous, in particular $|\mathscr{M}(w, w)| \leq C\|w\|_0^2$, where $\|\cdot\|_0$ denotes the L^2 norm. Note that for linear outputs, $\mathscr{M} = 0$.

The error bound procedure comprises the following five steps (for an alternative description see Appendix A).

Step 1

In the first step, the Galerkin finite element solution is computed on the working mesh: find $u_H = u_H^{\mathrm{R}} + \mathrm{i}u_H^{\mathrm{I}} \in Z_H^{\mathrm{D}}$ such that

$$E(u_H, v) = \langle f, v \rangle + \langle g^{\mathrm{N}}, v \rangle_{\mathrm{N}}, \quad \forall v \in Z_H. \tag{35}$$

The residual is also defined

$$R^u(v) \equiv \langle f, v \rangle + \langle g^{\mathrm{N}}, v \rangle_{\mathrm{N}} - E(u_H, v); \tag{36}$$

note that $R^u(v) = 0$, $\forall v \in Z_H$.

Step 2

In the second step, the adjoints are computed on the working mesh: find $\psi_H = \psi_H^{\mathrm{R}} + \mathrm{i}\psi_H^{\mathrm{I}} \in Z_H$ such that

$$E(v, \psi_H) = -\ell^{\mathscr{O}}(v), \quad \forall v \in Z_H. \tag{37}$$

The residual is also defined

$$R^{\psi}(v) \equiv -\overline{\ell^{\mathscr{O}}(v)} - \overline{E(v, \psi_H)}; \tag{38}$$

similar to Step 1, $R^{\psi}(v) = 0$, $\forall v \in Z_H$.

Step 3

In the third step, the *hybrid fluxes* are computed on the working mesh: find $p^u_H = p^{u\mathrm{R}}_H + \mathrm{i}p^{u\mathrm{I}}_H \in \mathscr{Q}_H$ and $p^{\psi}_H = p^{\psi\mathrm{R}}_H + \mathrm{i}p^{\psi\mathrm{I}}_H \in \mathscr{Q}_H$, such that

$$b(v, p_H^u) = R^u(v), \quad \forall v \in \hat{Z}_H, \tag{39}$$

$$b(v, p_H^\psi) = R^\psi(v), \quad \forall v \in \hat{Z}_H; \tag{40}$$

then $p_H^\pm = \kappa p_H^u \mp p_H^\psi$ is set, where $\kappa \in \mathbb{R}_+$ is a scaling parameter with respect to which optimization will be performed. The equilibration procedure is a complex version of that developed in [18], which is in turn based on earlier work in the energy norm context [20–22].

Step 4
In the fourth step, the *reconstructed errors* are computed on the decoupled truth space $\hat{Z}_h$: find $\hat{e}^u = \hat{e}^{u\mathrm{R}} + \mathrm{i}\hat{e}^{u\mathrm{I}} \in \hat{Z}_h$ and $\hat{e}^\psi = \hat{e}^{\psi\mathrm{R}} + \mathrm{i}\hat{e}^{\psi\mathrm{I}} \in \hat{Z}_h$, such that

$$2E_Y^s(\hat{e}^u, v) - R_H^u(v) + b(v, p_H^u) = 0, \quad \forall v \in \hat{Z}_h, \tag{41}$$

$$2E_Y^s(\hat{e}^\psi, v) - R_H^\psi(v) + b(v, p_H^\psi) = 0, \quad \forall v \in \hat{Z}_h; \tag{42}$$

then $\hat{e}^\pm = \hat{e}^u \mp (1/\kappa)\hat{e}^\psi$. It is important to note that Equations (41) and (42) correspond to local and uncoupled problems, and are thus very inexpensively solved.

Step 5
Finally, in the fifth step, the lower and upper bounds are computed as

$$s^- = \Re\{S(u_H)\} - \kappa E_Y^s(\hat{e}^-, \hat{e}^-), \tag{43}$$

$$s^+ = \Re\{S(u_H)\} + \kappa E_Y^s(\hat{e}^+, \hat{e}^+). \tag{44}$$

As described in [19], these lower and upper bounds can be readily optimized (maximized and minimized respectively) with respect to the scaling parameter κ by choosing $\kappa = \kappa^*$, with

$$\kappa^* = \sqrt{\frac{E_Y^s(\hat{e}^\psi, \hat{e}^\psi)}{E_Y^s(\hat{e}^u, \hat{e}^u)}}. \tag{45}$$

Note that, from (32), κ^* will necessarily be real.

3.3. Bounding properties

In order to prove that the estimators (43) and (44) are (asymptotically) lower and upper bounds respectively for $s_h = \Re\{S(u_h)\}$ (the non-linear output on the truth mesh), the field variable error is first introduced,

$$e = u_h - u_H, \tag{46}$$

which is the difference between the truth and working mesh approximations; note that $e \in Z_h$. Then, Equations (41) and (42) are summed to obtain the equation for the reconstructed error $\hat{e}^-$:

$$2\kappa E_Y^s(\hat{e}^-, v) - \kappa R_H^u(v) - R_H^\psi(v) + b(v, p_H^-) = 0, \quad \forall v \in \hat{Z}_h, \tag{47}$$

in which, since $Z_h \subset \hat{Z}_h$, one can choose $v = e$,

$$2\kappa E_Y^s(\hat{e}^-, e) - \kappa R_H^u(e) - R_H^\psi(e) + b(e, p_H^-) = 0. \tag{48}$$

Appealing to the expressions for R_H^u and R_H^ψ, and noting that $e \in Z_h$ (and hence $b(e, p_H^-) = 0$), it is found that

$$2\kappa E_Y^s(\hat{e}^-, e) - \kappa[\langle f, e\rangle + \langle g^{\mathrm{N}}, e\rangle_{\mathrm{N}} - E(u_H, e)] + \overline{\ell^{\mathcal{O}}(e)} + \overline{E(e, \psi_H)} = 0. \tag{49}$$

From the usual orthogonality condition, it is known that $E(e, v) = 0$, $\forall v \in Z_H$, and thus $\overline{E(e, \psi_H)} = 0$. Also, $E(u_h, v) = \langle f, v \rangle + \langle g^{\mathrm{N}}, v \rangle_{\mathrm{N}}$, $\forall v \in Z_h$, and hence $E(u_h, e) = \langle f, e \rangle + \langle g^{\mathrm{N}}, e \rangle_{\mathrm{N}}$. One thus obtains

$$2\kappa \overline{E_Y^s(\hat{e}^-, e)} - \kappa E(e, e) + \ell^{\mathscr{C}}(e) = 0, \tag{50}$$

and in particular

$$\Re\{2\kappa \overline{E_Y^s(\hat{e}^-, e)} - \kappa E(e, e) + \ell^{\mathscr{C}}(e)\} = 0. \tag{51}$$

Summing this last identity with (43), applying the Taylor expansion (34) and noting that

$$\Re\{2\overline{E_Y^s(\hat{e}^-, e)}\} = \overline{E_Y^s(\hat{e}^-, e)} + E_Y^s(\hat{e}^-, e) = E_Y^s(e, \hat{e}^-) + E_Y^s(\hat{e}^-, e), \tag{52}$$

one obtains

$$s^- = \Re\{S(u_h)\} - \kappa E_Y^s(e - \hat{e}^-, e - \hat{e}^-) - \kappa E_M^s(e, e) - \Re\{\mathscr{M}(e, e)\}, \tag{53}$$

which is the desired result.

Note that $\kappa E_M^s(e, e) + \Re\{\mathscr{M}(e, e)\} \leq C\|e\|_0^2$, which will vanish as $\mathscr{O}(H^4)$—much faster than $\kappa E_Y^s(e - \hat{e}^-, \mathrm{e} - \hat{e}^-)$, which will tend to zero as $\mathscr{O}(H^2)$. It then follows that, since E_Y^s is positive-definite, s^- will approach $\Re\{S(u_h)\}$ from below for H sufficiently small. A similar demonstration can be performed for the upper estimator (asymptotic upper bound) for $\Re\{S(u_h)\}$; in fact, the upper bound is simply the negative of the lower bound for $-S(u_h)$. In particular, you obtain

$$s^+ = \Re\{S(u_h)\} + \kappa E_Y^s(e - \hat{e}^+, e - \hat{e}^+) + \kappa E_M^s(e, e) - \Re\{\mathscr{M}(e, e)\}, \tag{54}$$

from which it is clear that s^+ will approach $\Re\{S(u_h)\}$ from above.

4. NUMERICAL EXAMPLES

This section presents several applications of the present procedure. All the examples involve the scattering of a plane wave by a rigid body, and thus there are no essential boundary conditions. It is assumed that the solution of the problem (1)–(4) is composed of a prescribed incident wave plus a scattered wave, $\tilde{u}_T = \tilde{u}_{(i)} + \tilde{u}$, where the incident wave is of the form $\tilde{u}_{(i)} = \Re\{u_{(i)}\, \mathrm{e}^{\mathrm{i}(\mathbf{k}^T\mathbf{x} + \omega t)}\}$. It is assumed that there are no sources in the domain ($\tilde{f} = 0$) and that perfect reflection obtains on the rigid body: $\partial \tilde{u}_T / \partial n = 0$ (or in terms of the incident wave, $\partial \tilde{u} / \partial n = -\partial \tilde{u}_{(i)} / \partial n$). The complex Helmholtz equation is thus: find u: $\bar{\Omega} \to \mathbb{C}$ such that

$$-\nabla^2 u - k^2 u = 0 \quad \text{in } \Omega, \tag{55}$$

$$\frac{\partial u}{\partial n} = -\mathrm{i}\mathbf{k}^T \hat{\mathbf{n}} u_{(i)}\, \mathrm{e}^{\mathrm{i}\mathbf{k}^T\mathbf{x}} \quad \text{on } \Gamma_{\mathrm{N}}, \tag{56}$$

$$\frac{\partial u}{\partial n} = -\mathrm{i}ku \quad \text{on } \Gamma_{\mathrm{R}}, \tag{57}$$

where k denotes the modulus of $\mathbf{k}$. The corresponding weak form is simply (14) with $f = g^{\mathrm{D}} = 0$ and $g^{\mathrm{N}} = -\mathrm{i}\mathbf{k}^T \mathbf{n} u_{(i)}\, e^{\mathrm{i}\mathbf{k}^T\mathbf{x}}$.

In the following examples the procedure is applied to three different engineering outputs. The first output is the normalized L^2 norm of the solution

$$S_1(v) = \frac{1}{A_\Omega} \int_\Omega v\bar{v} \, d\Omega, \tag{58}$$

where A_Ω is the area of the domain. To identify $\ell^\mathcal{O}$, appeal to (34),

$$S_1(u_H + w) = \frac{1}{A_\Omega} \int_\Omega (u_H + w)\overline{(u_H + w)} \, d\Omega = S_1(u_H) + \frac{1}{A_\Omega} \int_\Omega (u_H \bar{w} + \bar{u}_H w) \, d\Omega + S_1(w), \tag{59}$$

and thus

$$\ell^\mathcal{O}(w) = \frac{2}{A_\Omega} \int_\Omega \bar{u}_H w \, d\Omega, \quad \mathcal{M}(w, w) = S_1(w). \tag{60}$$

The second output is the modulus squared over a boundary strip $\Gamma^\mathcal{O}$,

$$S_2(v) = \frac{1}{\ell_{\Gamma^\mathcal{O}}} \int_{\Gamma^\mathcal{O}} v\bar{v} \, d\Gamma, \tag{61}$$

where $\ell_{\Gamma^\mathcal{O}}$ is the length of the boundary strip. This definition yields

$$\ell^\mathcal{O}(w) = \frac{2}{\ell_{\Gamma^\mathcal{O}}} \int_{\Gamma^\mathcal{O}} \bar{u}_H w \, d\Gamma, \quad \mathcal{M}(w, w) = S_2(w). \tag{62}$$

The third output is the real part of the solution, and thus

$$S_3(v) = \int_\Omega v \, d\Omega, \tag{63}$$

and $\ell^\mathcal{O}(w) = S_3(w)$, $\mathcal{M}(w, w) = 0$.

A square domain is considered in which an incident plane wave is travelling in the negative y-direction; inside this region there is a rigid body that scatters the incident wave. The radiation condition (57) is imposed on the exterior boundary and the reflection condition (56) on the rigid body surface. The boundary strip on which the output (61) is evaluated is the segment $\Gamma^\mathcal{O} = [(0.5, 1.0), (0.8, 1.0)]$. The geometry of the domain, the boundary conditions and the direction of the incident wave are depicted in Figure 2.

Triangulations $\mathcal{T}_{H_0,R}$ ($R = 1, 2, 4, 8, 16$) are introduced that are uniform refinements of the coarsest mesh, $\mathcal{T}_{H_0,1}$; even in $\mathcal{T}_{H_0,1}$ smaller elements are introduced near the rigid body to prevent dominance of the corner singularities. The truth mesh corresponds to $\mathcal{T}_{H_0,16}$; the working meshes correspond to $\mathcal{T}_{H_0,R}$ ($R = 1, 2, 4, 8$), for which the effective element size is denoted as $H \equiv 1/R$. Figure 3(a) and (b) show $\mathcal{T}_{H_0,1}$ and $\mathcal{T}_{H_0,16}$ respectively; Figure 3(c) shows graphically the decoupled truth mesh, which in effect defines $\hat{Z}_h$. Note that for the refinement values R chosen, $Z_H \subset Z_h \subset Z$ as required by the theory. In order to demonstrate the dependence of the results on the wave number, three wavenumber values are considered: $k = \pi$, $k = 3\pi$ and $k = 5\pi$. It is important to note that the coarsest mesh, $\mathcal{T}_{H_0,1}$, is not sufficiently fine to capture even the incident wave for $k = 3\pi$ or $k = 5\pi$.

First, the solution is computed on the truth mesh, u_h, from which the corresponding truth output, s_h, can be evaluated; recall that it is assumed that s_h differs negligibly from the exact value of the output, s. The columns of Figure 4 show the real part, the imaginary part and the modulus of the scattered wave, as well as the modulus of the total wave, for the three wavenumbers considered. In reality, we would not, of course, have access to u_h; we indulge here to demonstrate that s^+ and s^- are indeed bounds for s_h.

Next, based on $\mathcal{T}_{H_0,R}$ for $R = 1, 2, 4, 8$, the working mesh output s_H, the lower bound estimator s^- (43), the upper bound estimator s^+ (44), the bound predicted non-linear output

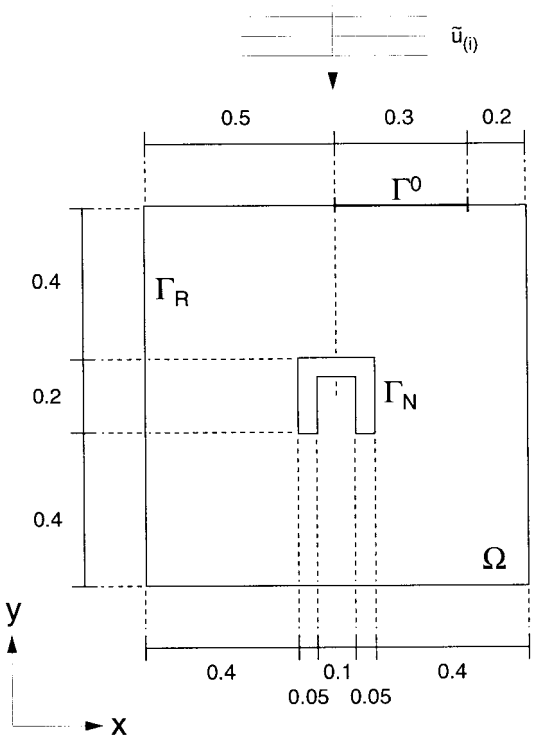

Figure 2. Geometry and boundary conditions for two-dimensional plane wave scattering by a rigid body.

value $s_H^{\text{pre}} = \frac{1}{2}(s^+ + s^-)$, and the (half) bound gap, $\Delta(\mathscr{T}_H) = \frac{1}{2}(s_h^+ - s_h^-)$, for each of the outputs (58), (61) and (63) and each of the three wavenumbers considered are computed. In reality, $\Delta(\mathscr{T}_H)$, which requires computations only on the decoupled fine mesh, would serve as the error bound on s_H^{pre}(or s_H); even more directly, s^- and s^+ would serve as delimiters for the range in which s_h must lie (at least for H sufficiently small). Often, depending on the particular problem, either the upper or the lower bound will be more relevant to the engineering design procedure.

Figure 5 presents, for the output $S_1(u)$ and for each of the wave numbers, s^-/s_h, s^+/s_h, s_H^{pre}/s_h and s_H/s_h as functions of H. The same plots are presented in Figures 6 and 7 for outputs $S_2(u)$ and $S_3(u)$ respectively. It is observed that bounds are obtained even for the largest values of H (in which there is clearly not enough resolution for the $k = 3\pi$ and $k = 5\pi$ waves). As expected, the bounds are less sharp with increasing wavenumber; for higher wavenumbers a finer mesh is needed. This behaviour can be better observed in Figure 8, in which the (half) bound gap, $\Delta(\mathscr{T}_h)$, is plotted as a function of H. Notice that quadratic converge is obtained, as might be expected from Equations (53) and (54) and earlier theory for the coercive case (Y. Maday and A.T. Patera, 'Numerical analysis of *a posteriori* finite elements bounds for linear-functional outputs', *Math. Models Methods Appl. Sci.*, submitted).

In order to demonstrate the influence of the initial mesh on the accuracy of the bounds, the bound calculations are repeated for the output (61), for $k = \pi$, for an initial mesh $\mathscr{T}_{H_{0,1}}$, which is modestly refined near $\Gamma^{\mathscr{O}}$. Figure 9(a) depicts the initial mesh $\mathscr{T}_{H_{0,1}}$; Figure 9(b) shows the new values for s^-/s_h, s^+/s_h, s_H^{pre}/s_h and s_H/s_h. Better bounds are obtained since the adjoint is more accurately approximated; the technique of [19] will automatically produce such an output optimal mesh.

5. CONCLUSIONS

The general formulation for *a posteriori* bounds for output functionals of partial differential equations has been extended to non-linear outputs of multi-dimensional complex exterior Helmholtz problems. In particular, it has been proven that the estimators obtained are asymptotically lower and upper bounds for the exact output (or more precisely, the truth output, s_h). Numerical examples verify the predicted quadratic convergence; furthermore, even for the largest value of H, strict bounds are obtained, indicating that the asymptotic qualifier is, in fact, rather weak. In many cases, the bounds are sufficiently sharp that relatively coarse

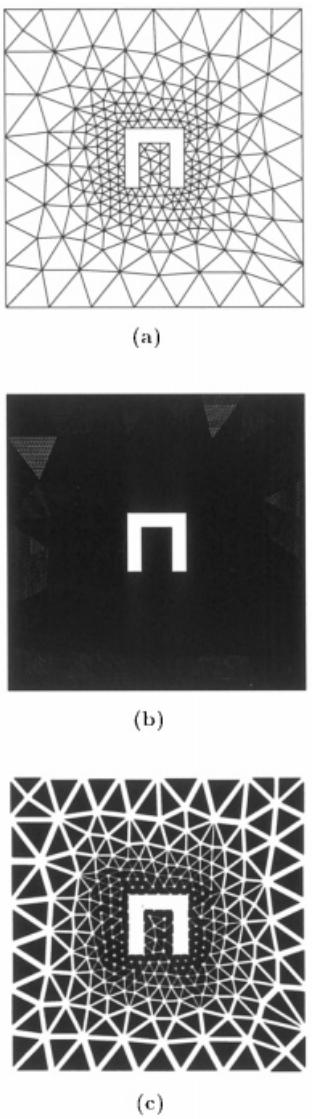

Figure 3. (a) Coarest mesh $\mathscr{T}_{H_0,1}$; (b) finest mesh $\mathscr{T}_{H_0,16}$; (c) mesh corresponding to the *broken* space $\hat{Z}_h$.

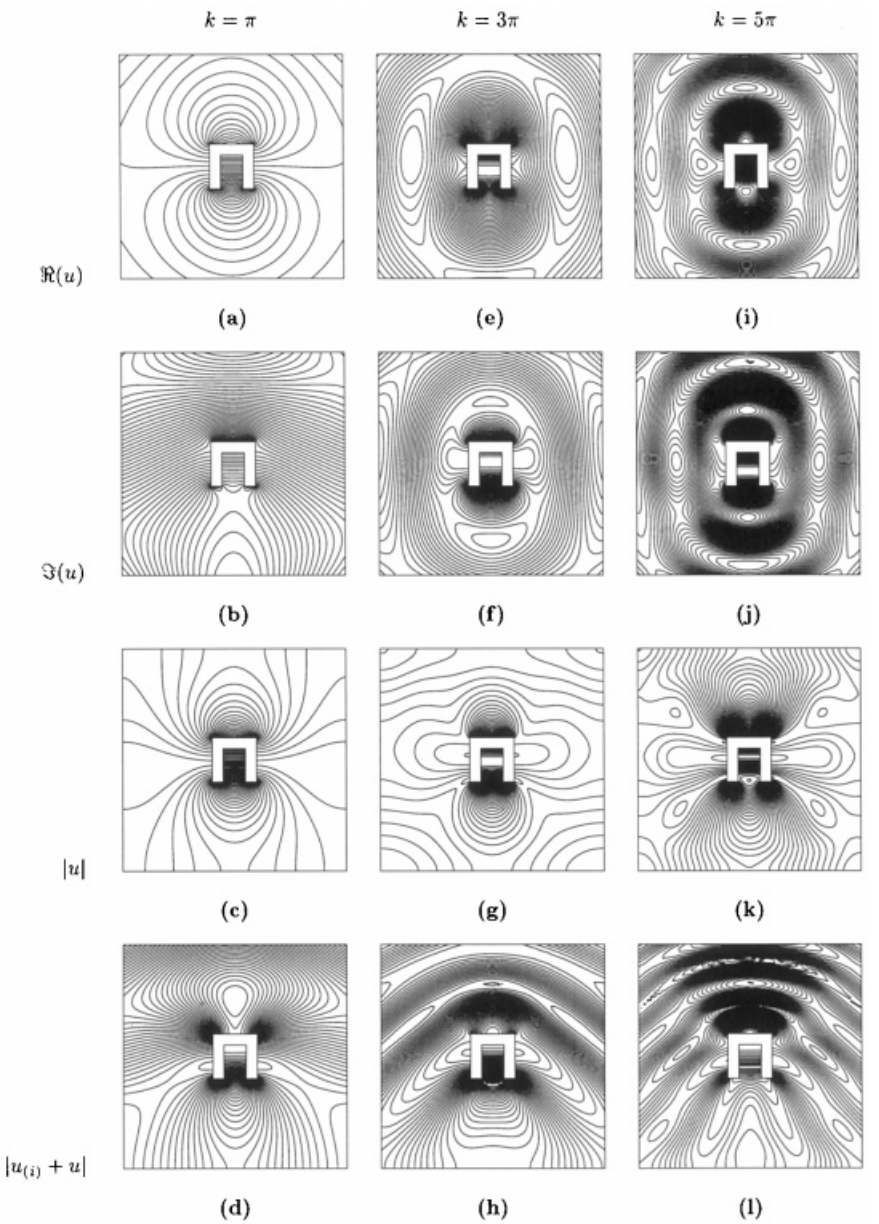

Figure 4. Contour plots of: $\Re(u)$ for (a) $k = \pi$, (e) $k = 3\pi$ and (i) $k = 5\pi$; $\Im(u)$ for (b) $k = \pi$, (f) $k = 3\pi$ and (j) $k = 5\pi$; $|u|$ for (c) $k = \pi$, (g) $k = 3\pi$ and (k) $k = 5\pi$; and $|u_{(i)} + u|$ for (d) $k = \pi$, (h) $k = 3\pi$ and (l) $k = 5\pi$.

meshes produce acceptable results; whereas typically the coarse mesh would not be trusted, the error bounds permit their safe application—thus providing both certainty and efficiency. Efficiency can be further improved by considering the adaptive procedures of [19].

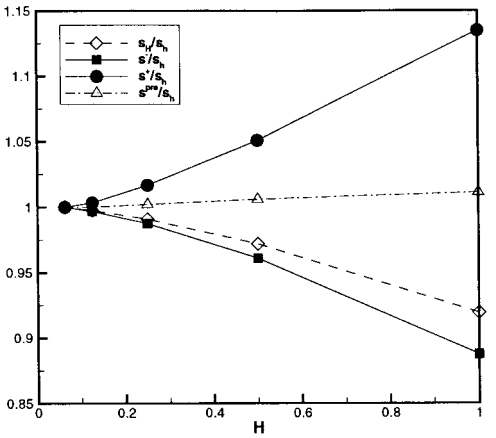

(a)

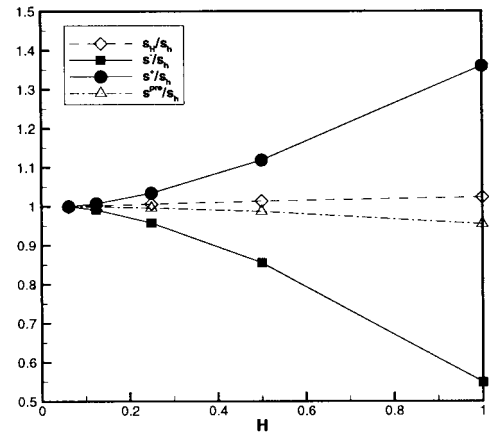

(b)

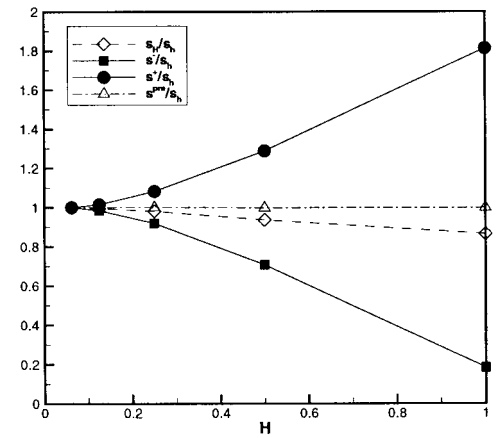

(c)

Figure 5. Plots of s^-/s_h, s^+/s_h, s_H^{pre}/s_h and s_H/s_h for $S_1(u)$ and (a) $k=\pi$, (b) $k=3\pi$ and (c) $k=5\pi$.

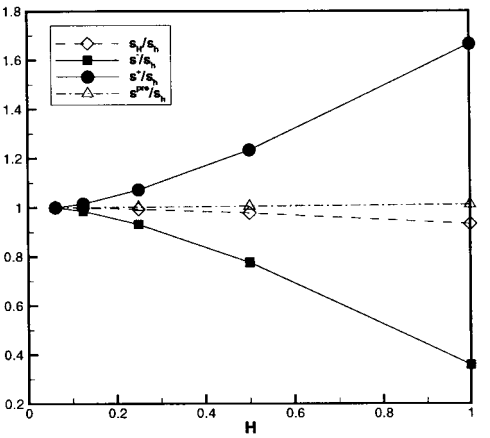

(a)

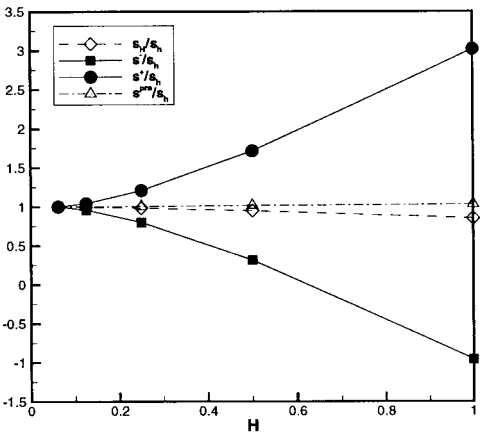

(b)

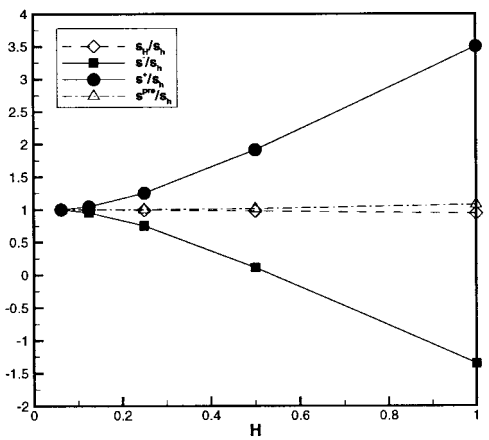

(c)

Figure 6. Plots of s^-/s_h, s^+/s_h, s_H^{pre}/s_h and s_H/s_h for $S_2(u)$ and (a) $k=\pi$, (b) $k=3\pi$ and (c) $k=5\pi$.

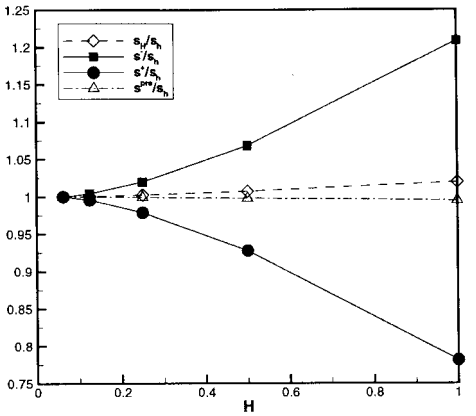

(a)

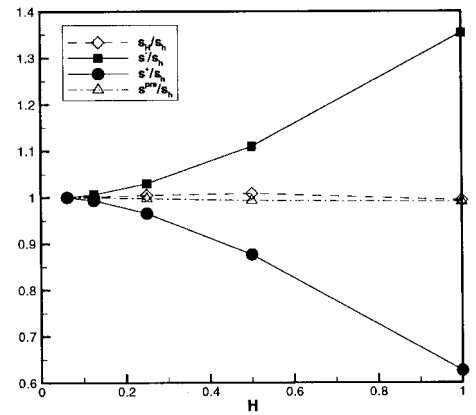

(b)

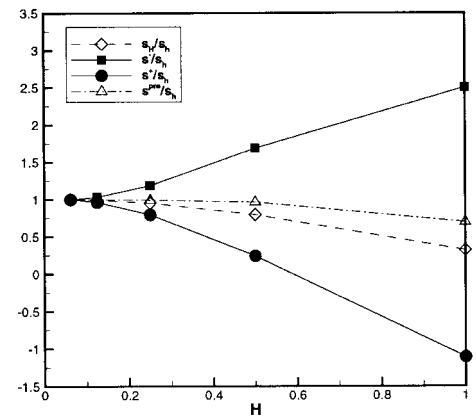

(c)

Figure 7. Plots of s^-/s_h, s^+/s_h, s_H^{pre}/s_h and s_H/s_h for $S_3(u)$ and (a) $k=\pi$, (b) $k=3\pi$ and (c) $k=5\pi$. Note that $\Re\{S_3(u)\}$ is negative, and hence the bounds *appear* reversed.

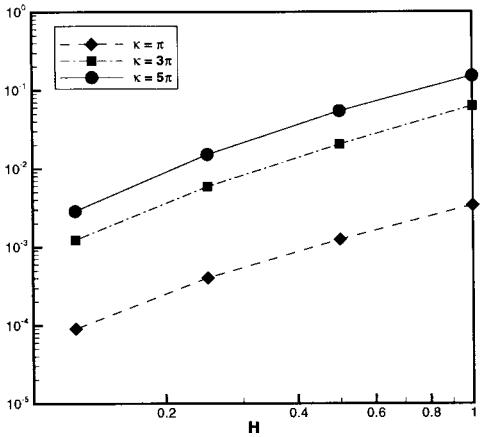

(a)

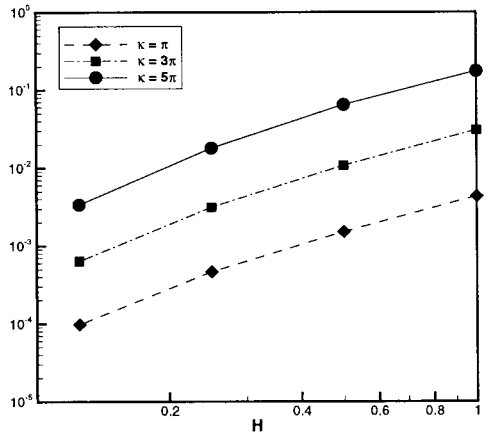

(b)

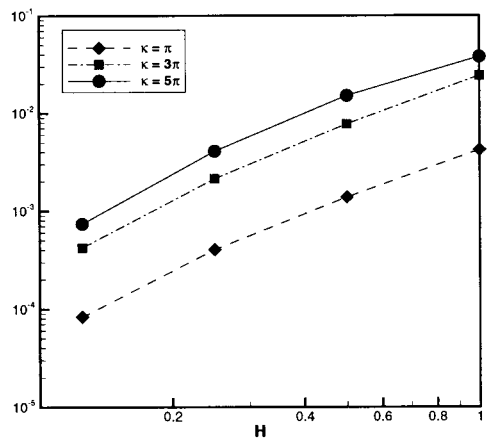

(c)

Figure 8. Plots of $\Delta(\mathscr{T}_h)$ for (a) $S_1(u)$, (b) $S_2(u)$ and (c) $S_3(u)$.

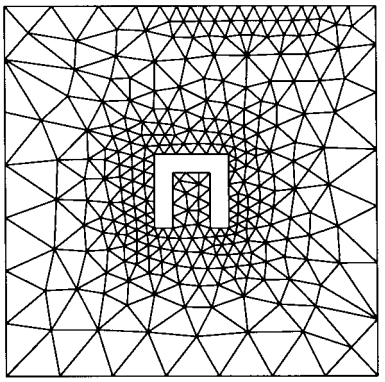

(a)

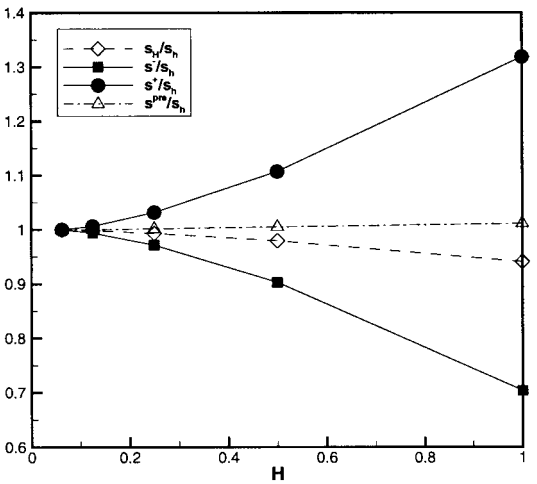

(b)

Figure 9. (a) Modified mesh; (b) plots of s^-/s_h, s^+/s_h, s_H^{pre}/s_h and s_H/s_h for $S_2(u)$ and $k=\pi$ for the modified mesh.

ACKNOWLEDGMENTS

This work was supported by NASA Grants NAG1-1978, NAG1-1587 and NAG4-105, DARPA and ONR Grant N00014-91-J-1889, and AFOSR Grant F49620-97-1-0052. J. Sarrate has been supported by the Comissionat per a Universitats i Recerca of the Generalitat de Catalunya.

APPENDIX A

It is shown here how the bound formulation can also be developed in terms of product spaces of real functions. To begin, the product space $H^1(\mathscr{D}) \times H^1(\mathscr{D})$ is considered, and

$$\tilde{X}(\mathscr{D}) = \{(\alpha, \beta) \in H^1(\mathscr{D}) \times H^1(\mathscr{D}):\ \alpha + \mathrm{i}\beta \in \tilde{Z}(\mathscr{D})\} \tag{64}$$

is defined and similarly

$$X = \{(\alpha, \beta) \in \tilde{X}(\Omega):\ \alpha + \mathrm{i}\beta \in Z\}, \tag{65}$$

$$X^{\mathrm{D}} = \{(\alpha, \beta) \in \tilde{X}(\Omega):\ \alpha + \mathrm{i}\beta \in Z^{\mathrm{D}}\}. \tag{66}$$

Then a bilinear form is defined: $\mathscr{B}:\ \tilde{X}(\Omega) \times \tilde{X}(\Omega) \to \mathbb{R}$ as

$$\mathscr{B}((\alpha, \beta), (\phi, \mu)) \equiv a(\alpha, \phi) + a(\beta, \mu) - m(\alpha, \phi) - m(\beta, \mu) + p(\alpha, \mu) - p(\beta, \phi) - \langle f^{\mathrm{R}}, \phi \rangle - \langle f^{\mathrm{I}}, \mu \rangle - \langle g^{\mathrm{NR}}, \phi \rangle_{\mathrm{N}} - \langle g^{\mathrm{NI}}, \mu \rangle_{\mathrm{N}}, \tag{67}$$

where the bilinear forms (16)–(18) and duality pairings (19)–(20) are now defined for real functions. The solution of problem (14), $u = u^{\mathrm{R}} + \mathrm{i}u^{\mathrm{I}}$, can thus be found by solving the following problem: find $(u^{\mathrm{R}}, u^{\mathrm{I}}) \in X^{\mathrm{D}}$ such that

$$\mathscr{B}((u^{\mathrm{R}}, u^{\mathrm{I}}), (\phi, \mu)) = 0, \quad \forall (\phi, \mu) \in X. \tag{68}$$

To see that (68) and (14) are, in fact, equivalent, it is noted that if $\phi = v^{\mathrm{R}}$ and $\mu = v^{\mathrm{I}}$ are set, (68) reduces to the real part of (14); whereas if $\phi = -v^{\mathrm{I}}$ and $\mu = v^{\mathrm{R}}$ are set, then (68) reduces to the imaginary part of (14). From this point of view, it is understood that problem (14) contains some redundancy, since the real and imaginary parts of the equation must be satisfied for the real and imaginary parts of the test functions.

In order to interpret the five steps of the procedure (35)–(44) in terms of spaces of real functions, there is a need to introduce the definitions of the equivalent real spaces first. Analogous to Z_δ, Z_δ^{D} and $\hat{Z}_\delta$, (21), (22) and (25), the following are defined:

$$X_\delta = \{(\alpha, \beta):\ \alpha|_{T_\delta} \in \mathbf{P}_1(T_\delta),\ \beta|_{T_\delta} \in \mathbf{P}_1(T_\delta),\ \forall T_\delta \in \mathscr{T}_\delta\} \cap X, \tag{69}$$

$$X_\delta^{\mathrm{D}} = \{(\alpha, \beta):\ \alpha|_{T_\delta} \in \mathbf{P}_1(T_\delta),\ \beta|_{T_\delta} \in \mathbf{P}_1(T_\delta),\ \forall T_\delta \in \mathscr{T}_\delta\} \cap X^{\mathrm{D}}, \tag{70}$$

$$\hat{X}_\delta = \{(\alpha, \beta)|_{T_H} \in \tilde{X}(T_H),\ \forall T_H \in \mathscr{T}_H:\ \alpha|_{T_\delta} \in \mathbf{P}_1(T_\delta),\ \beta|_{T_\delta} \in \mathbf{P}_1(T_\delta),\ \forall T_\delta \in \mathscr{T}_\delta\}. \tag{71}$$

Also, the real counterpart of the space $\mathscr{Q}_H$ is defined as $Q_H = W_H \times W_H$, where

$$W_H = \{q:\ q|_\gamma \in \mathbf{P}_1(\gamma),\ \forall \gamma \in \mathscr{E}(\mathscr{T}_H),\ \text{and}\ q|_{\Gamma_{\mathrm{N}}} = q|_{\Gamma_{\mathrm{R}}} = 0\}. \tag{72}$$

The continuity bilinear form $b(\cdot, \cdot)$ of (27) is also now defined over real functions as b: $\hat{X}_h \times Q_H \to \mathbb{R}$, where

$$b((\alpha, \beta), (q_\alpha, q_\beta)) = \sum_{\gamma \in \mathscr{E}(\mathscr{T}_H)} \int_\gamma [\alpha]_\gamma\, q_\alpha|_\gamma \, \mathrm{d}\Gamma + \int_\gamma [\beta]_\gamma\, q_\beta|_\gamma \, \mathrm{d}\Gamma. \tag{73}$$

It remains only to modify properly the definition of the non-linear output: set $s = \check{S}((\alpha, \beta))$, where $\check{S}:\ \tilde{X}(\Omega) \to \mathbb{R}$ such that $\check{S}((\alpha, \beta)) = \Re\{S(\alpha + \mathrm{i}\beta)\}$.

This problem is now defined over spaces of real functions and the bound formulation presented in [16] is directly applicable. Following that notation, and since $\mathscr{B}$ is bilinear, we have

$$E((\alpha, \beta), (\phi, \mu)) = \alpha(\alpha, \phi) + a(\beta, \mu) - m(\alpha, \phi) - m(\beta, \mu) + p(\alpha, \mu) - p(\beta, \phi). \tag{74}$$

As usual, E is decomposed into its symmetric and skew-symmetric parts, $E = E^s + E^a$, where

$$E^s((\alpha, \beta), (\phi, \mu)) \equiv a(\alpha, \phi) + a(\beta, \mu) - m(\alpha, \phi) - m(\beta, \mu), \tag{75}$$

$$E^a((\alpha, \beta), (\phi, \mu)) \equiv p(\alpha, \mu) - p(\beta, \phi). \tag{76}$$

The symmetric part is then further decomposed as $E^s \equiv E^s_Y + E^s_M$, where

$$E^s_Y((\alpha,\beta),(\phi,\mu)) \equiv a(\alpha,\phi) + a(\beta,\mu), \tag{77}$$

$$E^s_M((\alpha,\beta),(\phi,\mu)) \equiv -m(\alpha,\phi) - m(\beta,\mu). \tag{78}$$

Finally, write

$$\check{S}((u^{\mathrm{R}},u^{\mathrm{I}})+(\alpha,\beta)) = \check{S}((u^{\mathrm{R}},u^{\mathrm{I}})+\check{\ell}^{\mathscr{O}}(\alpha,\beta)) + \check{\mathscr{M}}((\alpha^{\mathrm{R}},\beta^{\mathrm{I}}),(\alpha,\beta)), \tag{79}$$

such that $\check{\ell}^{\mathscr{O}}((\alpha,\beta)) = \Re\{\ell^{\mathscr{O}}(\alpha+\mathrm{i}\beta)\}$, and $\check{\mathscr{M}}((\alpha,\beta),(\alpha,\beta)) = \Re\{\mathscr{M}(\alpha+\mathrm{i}\beta,\alpha+\mathrm{i}\beta)\}$.

With these definitions, the estimator procedure comprises the following five steps.

Step 1

Compute the finite element solution $(u^{\mathrm{R}}_H, u^{\mathrm{I}}_H)\in X^H_{\mathrm{D}}$ such that

$$E((u^{\mathrm{R}}_H,u^{\mathrm{I}}_H),(\phi,\mu)) = \langle f^{\mathrm{R}},\phi\rangle + \langle f^{\mathrm{I}},\mu\rangle + \langle g^{\mathrm{NR}},\phi\rangle_{\mathrm{N}} + \langle g^{\mathrm{NI}},\mu\rangle_{\mathrm{N}}, \quad \forall(\phi,\mu)\in X_H. \tag{80}$$

Also, the residual is defined as

$$R^u(\phi,\mu) \equiv \langle f^{\mathrm{R}},\phi\rangle + \langle f^{\mathrm{I}},\mu\rangle + \langle g^{\mathrm{NR}},\mu\rangle_{\mathrm{N}} + \langle g^{\mathrm{NI}},\mu\rangle_{\mathrm{N}} - E((u^{\mathrm{R}}_H,u^{\mathrm{I}}_H),(\phi,\mu)). \tag{81}$$

Step 2

Compute the adjoints $(\psi^{\mathrm{R}}_H,\psi^{\mathrm{I}}_H)\in X_H$ such that

$$E((\phi,\mu),(\psi^{\mathrm{R}}_H,\psi^{\mathrm{I}}_H)) = -\check{\ell}^{\mathscr{O}}((\phi,\mu)), \quad \forall(\phi,\mu)\in X_H. \tag{82}$$

Also, the residual is defined as

$$R^{\psi}(\phi,\mu) \equiv -\check{\ell}^{\mathscr{O}}((\phi,\mu)) - E((\phi,\mu),(\psi^{\mathrm{R}}_H,\psi^{\mathrm{I}}_H)). \tag{83}$$

Step 3

Compute the hybrid fluxes $(p^{u\mathrm{R}}_H, p^{u\mathrm{I}}_H)\in Q_H$ and $(p^{\psi\mathrm{R}}_H, p^{\psi\mathrm{I}}_H)\in Q_H$, such that

$$b((\phi,\mu),(p^{u\mathrm{R}}_H,p^{u\mathrm{I}}_H)) = R^u(\phi,\mu), \quad \forall(\phi,\mu)\in\hat{X}_H, \tag{84}$$

$$b((\phi,\mu),(p^{\psi\mathrm{R}}_H,p^{\psi\mathrm{I}}_H)) = R^{\psi}(\phi,\mu), \quad \forall(\phi,\mu)\in\hat{X}_H; \tag{85}$$

then set $(p^{\pm\mathrm{R}}_H, p^{\pm\mathrm{I}}_H) = \kappa(p^{u\mathrm{R}}_H, p^{u\mathrm{I}}_H) \mp (p^{\psi\mathrm{R}}_H, p^{\psi\mathrm{I}}_H)$, where $\kappa\in\mathbb{R}_+$ is the scaling parameter.

Step 4

Compute the reconstructed errors: find $(\hat{e}^{u\mathrm{R}},\hat{e}^{u\mathrm{I}})\in\hat{X}_h$ and $(\hat{e}^{\psi\mathrm{R}},\hat{e}^{\psi\mathrm{I}})\in\hat{X}_h$ such that

$$2E^s_Y((\hat{e}^{u\mathrm{R}},\hat{e}^{u\mathrm{I}}),(\phi,\mu)) - R^u_H(\phi,\mu) + b((\phi,\mu),(p^{u\mathrm{R}}_H,p^{u\mathrm{I}}_H)) = 0, \quad \forall(\phi,\mu)\in\hat{X}_h, \tag{86}$$

$$2E^s_Y((\hat{e}^{\psi\mathrm{R}},\hat{e}^{\psi\mathrm{I}}),(\phi,\mu)) - R^{\psi}_H(\phi,\mu) + b((\phi,\mu),(p^{\psi\mathrm{R}}_H,p^{\psi\mathrm{I}}_H)) = 0, \quad \forall(\phi,\mu)\in\hat{X}_h; \tag{87}$$

then set $(\hat{e}^{\pm\mathrm{R}},\hat{e}^{\pm\mathrm{I}}) = (\hat{e}^{u\mathrm{R}},\hat{e}^{u\mathrm{I}}) \mp (1/\kappa)(\hat{e}^{\psi\mathrm{R}},\hat{e}^{\psi\mathrm{I}})$.

Step 5

Compute lower and upper bounds

$$s^- = \check{S}((u^{\mathrm{R}}_H,u^{\mathrm{I}}_H)) - \kappa E^s_Y((\hat{e}^{-\mathrm{R}},\hat{e}^{-\mathrm{I}}),(\hat{e}^{-\mathrm{R}},\hat{e}^{-\mathrm{I}})), \tag{88}$$

$$s^+ = \check{S}((u^{\mathrm{R}}_H,u^{\mathrm{I}}_H)) + \kappa E^s_Y((\hat{e}^{+\mathrm{R}},\hat{e}^{+\mathrm{I}}),(\hat{e}^{+\mathrm{R}},\hat{e}^{+\mathrm{I}})). \tag{89}$$

As it has been proved in [16] for real function spaces, these lower and upper estimators are, in fact, upper and lower bounds for $\check{S}((u^{\mathrm{R}}_h,u^{\mathrm{I}}_h))$ for H sufficiently small.

REFERENCES

1. K. Kashiyama and M. Sakuraba, 'Adaptive boundary-type finite element method for wave diffraction–refraction in harbours', *Comput. Methods Appl. Mech. Eng.*, **112**, 185–197 (1994).
2. M.O. Bristeau, R. Glowinsky and J. Periaux, 'Using exact controllability to solve the Helmholtz equation at high wave numbers', *Proc. 2nd Int. Conf. on Mathematics and Numerical Aspects of Wave Propagation*, SIAM, 1993.
3. J.R Stewart, 'Adaptive finite element method for the Helmholtz equation in exterior domains', *Ph.D. Thesis*, Division of Applied Mechanics, Stanford University, Stanford, CA, 1995.
4. J.R Stewart and J.R. Hughes, 'Explicit residual-based *a posteriori* error estimation for finite element discretizations of the Helmholtz equation: computation of the constant and new measures of the error estimator quality', *Comput. Methods Appl. Mech. Eng.*, **131**, 335–363 (1996).
5. S. Amini and K. Chen, 'Iterative solution of boundary element equations for the exterior acoustic problem', *J. Vibr. Acoust.*, **112**, 257–262 (1990).
6. L. Demkowicz and J.T. Oden, 'Recent progress on application of hp-adaptive BE/FE methods to elastic scattering', *Int. J. Numer. Methods Eng.*, **37**, 2893–2910 (1994).
7. M. Kamon, M.J. Tsuk and J.K. White, 'FASTHENRY: A multipole accelerated 3D inductance extraction program', *IEEE Trans. Microwave Theory Technol.*, **42**, 1750–1758 (1994).
8. P. Bettess, 'Infinite elements', *Int. J. Numer. Methods Eng.*, **11**, 53–64 (1977).
9. D. Givoli and J.B. Keller, 'Non-reflecting boundary conditions for elastic waves', *Wave Motion*, **12**, 261–279 (1990).
10. Y. Saad and M.H. Schultz, 'GMRES: A generalized minimal residual algorithm for solving nonsymmetric linear systems', *SIAM J. Sci. Stat. Comput.*, **7**, 856–869 (1986).
11. A.H. Schatz, 'An observation concerning Ritz–Galerkin methods with indefinite bilinear forms', *Math. Comp.*, **128**, 959–962 (1974).
12. I. Babuska, F. Ihlenburg, T. Strouboulis and S.K. Gangaraj, '*A posteriori* error estimator for finite element solutions of Helmholtz equation, Part II. Estimation of the pollution error', *Int. J. Numer. Methods Eng.*, **40**, 3883–3900 (1997).
13. C. Johnson and P. Hansbo, 'Adaptive finite element methods in computational mechanics', *Comput. Methods Appl. Mech. Eng.*, **101**, 143–181 (1992).
14. F. Ihlenburg and I. Babuska, 'Finite element solution of the Helmholtz equation with high wave number, Part I. The *h*-version of the FEM', *Comput. Math. Appl.*, **30**, 9–37 (1995).
15. R. Becker and R. Rannacher, 'Weighted *a posteriori* error control in finite element methods', *IWR Preprint 96-1 (SFB 359)*, Heidelberg, 1996.
16. Y. Maday, A.T. Patera and J. Peraire, 'A general formulation for *a posteriori* bounds for output functionals of partial differential equations; application to the eigenvalue problem', *C. R. Acad. Sci. Paris*, to appear.
17. M. Paraschivoiu, 'A posteriori finite element bounds for linear-functional outputs of coercive partial differential equations and of the Stokes problem', *Ph.D. Thesis*, Department of Mechanical Engineering, M.I.T., October, 1997.
18. M. Paraschivoiu, J. Peraire and A.T. Patera, '*A posteriori* finite element bounds for linear-functional outputs of elliptic partial differential equations', *Comput. Methods Appl. Mech. Eng.*, **150**, 289–312 (1997).
19. J. Peraire and A.T. Patera, 'Bounds for linear-functionals outputs of coercive partial differential equations: local indicators and adaptive refinement', in P. Ladeveze and J.T. Oden (eds.), *Proceedings of the Workshop on New Advances in Adaptive Computational Methods in Mechanics*, Cachan, France, Elsevier, Amsterdam, 1997.
20. R.E. Bank and A. Weiser, 'Some *a posteriori* error estimators for elliptic partial differential equations', *Math. Comput.*, **44**, 283–301 (1985).
21. M. Ainsworth and J.T. Oden, 'A unified approach to *a posteriori* error estimation using element residual methods', *Numer. Math.*, **65**, 23–50 (1993).
22. P. Ladeveze and D. Leguillon, 'Error estimation procedures in the finite element method and applications', *SIAM J. Numer. Anal.*, **20**, 485–509 (1983).
23. M. Ainsworth and J.T. Oden, '*A posteriori* error estimation in finite element analysis', *Comput. Methods Appl. Mech. Eng.*, **142**, 1–8 (1997).
24. J. Peraire and A.T. Patera, 'Asymptotic *a posteriori* finite element bounds for the outputs of non coercive problems: the Helmholtz and Burgers equations', *Comput. Methods Appl. Mech. Eng.*, **171**, 77–86 (1999).
25. L. Machiels, A.T. Patera, J. Peraire and Y. Maday, 'A general framework for finite element *a posteriori* error control: application to linear and non-linear convection-dominated problems', *ICFD Conference on Numerical Methods for Fluid Dynamics*, Oxford, UK, 1998.
26. R.A. Adams, *Sobolev Spaces*, Academic Press, New York, 1975.

